A real-coded evolutionary algorithm-based registration approach for forensic identification using the radiographic comparison of frontal sinuses

Óscar Gómez*†‡, Pablo Mesejo*†‡, Óscar Ibáñez†‡, Andrea Valsecchi†‡ and Óscar Cordón*†
*Dept. of Computer Science and Artificial Intelligence, University of Granada, Spain.
†Andalusian Research Institute DaSCI, University of Granada, Spain.
‡Panacea Cooperative Research S. Coop., Ponferrada, Spain.
Email: ogomez@decsai.ugr.es, pmesejo@decsai.ugr.es, oscar.ibanez@panacea-coop.com,
valsecchi.andrea@panacea-coop.com, ocordon@decsai.ugr.es

***Abstract*—Comparative radiography is the forensic anthropology technique in which ante-mortem (AM) and post-mortem (PM) radiographic materials (e.g., X-ray images or CTs) are compared in order to determine the identity of a deceased human being. One of the most commonly used anatomical structures in comparative radiography are the frontal sinuses. The frontal sinuses are osseous cavities located in the skull, which are used in forensic identification tasks due to their singularity and high identification power. In order to automate the comparison of frontal sinuses in AM and PM materials, it is necessary to perform the registration of these materials (i.e., it is necessary to carry out the alignment of these anatomical regions). However, the manual alignment of these structures is a time-consuming and subjective process. In order to tackle this problem, this paper presents an automatic frontal sinuses registration method in comparative radiography using real-coded evolutionary algorithms (RCEAs). The task is formulated as a 2D-3D image registration problem using a 9 Degrees of Freedom perspective transformation model; two RCEAs (DE and MVMO-SH) are compared in the minimization of the registration cost function, and the best of them (MVMO-SH) is applied to an identification scenario including 50 X-ray images and 50 CTs. The results obtained show that the proposed automatic identification system is able to filter more than 80% of the sample.**

***Index Terms*—Biomedical Image Registration, Forensic Identification, Comparative Radiography, Frontal Sinuses, Real-Coded Evolutionary Algorithms, Mean Variance Mapping Optimization, Differential Evolution**

I. Introduction

Comparative radiography (CR) [1] is a forensic identification technique based on the comparison of skeletal structures in ante-mortem (AM) and post-mortem (PM) radiographs. Since the discovery of X-rays by Roentgen in 1895 [2], forensic experts have made use of radiographic images as evidence in their endeavour (e.g. bullet analysis [3], age estimation [4], and forensic identification [5]). During the first decades of the twentieth century, the use of X-rays as a method of positive identification gradually consolidated in scientific literature. In fact, in 1949, CR techniques played a crucial role in the identification of people involved in the Noronic ship's disaster, proving their importance for identification and being included in many mass disaster identification protocols [6]. Nowadays, CR is still employed in many forensic identification scenarios. For instance, the Michigan State University Forensic Anthropology Laboratory (MSUFAL) performed 193 identifications using this approach between 2002 and 2015 [7].

Several bones and cavities have been reported as useful for candidate short-listing or positive identification based on their individuality and uniqueness [8]. In particular, frontal sinuses (see Fig. 1) are widely recognized as a useful and reliable method of identification [9], fulfilling the Daubert criteria [10][1]. Frontal sinuses are only absent in 4% of the population and are maintained unchanged during the rest of the life [12]. Although, rarely, some external factors such as traumatisms can change slightly their morphology, frontal sinuses are considered as a skeleton fingerprint. Their utilization for CR-based identification was first reported in 1926 by comparing their morphology in AM and PM radiographs [13]. Nowadays, CR identification based on frontal sinuses is widely accepted by the forensic community, and many works have reported their utility via image comparison to establish positive identification [14]–[16].

CR techniques have lower cost and time requirements in comparison to DNA analysis, which are crucial factors in mass disaster victim identification scenarios. However, the application of CR requires the superimposition of the AM and PM data for their visual comparison by producing PM radiographs simulating the AM ones in scope and projection. This is a time-consuming trial-and-error process, that relies completely on the skills and experience of the analyst. Furthermore, the utility of the method is reduced because of the errors related to analysts' fatigue and subjectivity. There is thus a need to automate CR-based identification methods.

The automation of the CR's superimposition process is complex and computationally expensive (see Section II for further details). This is due to several reasons, such as the unknown set-up of the AM radiograph, the fact that image

[1]The Daubert criteria [11] determine whether evidence is admissible in a court of law. An identification method fulfills the Daubert criteria when: (1) it is testable and peer reviewed; (2) it possesses known potential error rates; and (3) it is accepted by the forensic community.

978-1-7281-6929-3/20/$31.00 ©2020 IEEE

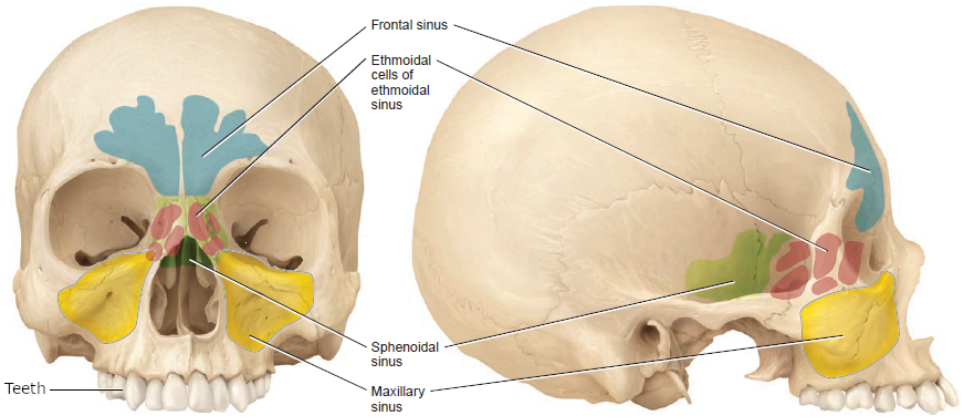

Fig. 1. Frontal sinuses (in light blue): one of the most relevant skeletal structures for CR-based identification. Images extracted from [17].

intensities are not reliable or even not captured, and the high multimodality of the search space configured by the registration framework, among others. These reasons make classic 3D-2D image registration (IR) techniques [18] not suitable for CR, and more sophisticated techniques should be considered in order to solve it, as real-coded evolutionary algorithms (RCEAs). In particular, the current state-of-the-art approach for CR follows an evolutionary 3D-2D IR methodology based on Differential Evolution (DE) [19]. In [19], several numerical optimization methods based on both linear search (Nelder-Mead, BFGS, LBFGS) and trust-region (Levenberg-Marquardt, BOBYQA) were tested to solve our IR problem, but their performance was insufficient. DE is taken as comparative reference in the experimentation of this paper, but we also introduce a competitor approach termed Mean-variance mapping optimization (MVMO) [20]. The reason to include this RCEA can be found on its excellent performance and robustness when tackling computationally expensive real-coded optimization problems as 3D-2D IR for CR is an instance of these kinds of problems. MVMO is in top positions in expensive optimization competitions, such as IEEE CEC 2013 [21], 2014 [22], 2015 [23], 2016 [24], and 2018 [25].

This paper presents an automatic frontal sinuses registration method in CR using RCEAs. The contribution of this research work is twofold. First, this is the first time that the problem is posed as a 3D-2D IR problem using a 9 Degrees of Freedom (9-DoF) perspective transformation model (a more complete model than the one previously employed [19]). Second, we employ a novel RCEA (MVMO-SH) that allows us to achieve state-of-the-art results in the IR-based CR problem and, therefore, up to our knowledge, it represents the most accurate automatic CR identification system available nowadays.

The rest of the paper is structured as follows. Section II briefly reviews the current state of the art in IR for CR. Section III describes our proposal to tackle the 3D bone scan-2D radiograph superimposition problem (9-DoF registration model and MVMO-SH). Section IV presents experiments and results obtained. The main conclusions are in Section V.

II. Background and Related Works

IR [18] is the process of aligning two or more images of the same or different dimensionalities into one coordinate system. 3D-2D IR approaches (e.g., Computed Tomographies (CTs)-radiograph or 3D surface mode-radiograph in CR) are classified into intensity-based and feature-based. Intensity-based methods compare intensities [18] of a 2D projection of the volumetric image with a fixed 2D image. However, one crucial consideration in any automatic method for CR is that the intensity level could have changed between the AM and the PM images as the bone density changes within the individual through time (due to factors as aging, osteoporosis, and the PM interval). Additionally, the intensity information varies depending on the X-ray acquisition protocols, devices employed, and cannot be acquired by 3D surface scans, which are being increasingly used by forensic labs [26] to scan PM "clean" bones due to their great availability and low cost, while just a few of them can afford a CT scan.

The former limitations lead to feature-based approaches. Feature-based IR methods minimize the distance between geometrical features to be segmented in both images. Forensic anthropologists consider bone morphology (silhouette) a reliable marker for performing the CR-based identification to compare radiographs of frontal sinuses [27], clavicles [28], and patellae [29]. However, these works cannot be considered as automatic IR methods since they only compare silhouettes using elliptical Fourier analysis [30]. The former one is based on the comparison of AM radiograph with a PM radiograph. The latter two, in contrast, are based on the comparison of the AM radiograph with a set of a predefined 2D projected images obtained through the rotation of 3D surface models acquired with a 3D laser range scanner. However, none of these completely automate the search for the best possible 2D projection of the PM 3D surface model of the bone.

Another important consideration about 3D-2D IR methods for medical domains [31] is that most of them are designed for a controllable set-up. Therefore, they can assume a calibrated case where the parameters related to the perspective distortions

are known, and only considering the parameters related to translations and rotations (6 DoF), and with a initialization pose close to the ground truth (GT) pose (i.e. a maximum target registration error [] of 16 mm in [31], etc). However, these assumptions are not suitable for CR since the AM radiograph was taken in an unknown pose with an unknown radiograph device. Therefore, the search for the optimal solution in the CR scenario is more complex. There are a few exceptions such as Feldman et al. [32], that proposed a 3D-2D IR method based on the silhouette that does not rely on assumptions about the initial pose by using free-form curves and surfaces, but it is only applicable in the calibrated case (6-DoF).

IR methods based on RCEAs, a.k.a. evolutionary IR methods, have demonstrated to overcome some of these drawbacks in others IR problems [33]. In particular, Gómez et al. [19] proposed an evolutionary 3D-2D IR approach for CR based on the bone or cavity silhouette. It automatizes the search of the best possible 2D projection of the PM 3D surface model of the bone (either obtained using a 3D scanner or segmented from a PM CT), and it does not consider any assumption on the initialization or the main parameter related to the perspective distortions in radiographs (i.e. the source to image distance, a.k.a. SID). This proposal is based on the use of DE [34], a modification of the DICE metric [35] that considers occlusion regions (which are regions hard to segment either because of the fuzzy borders of the bone or occlusions caused by other overlapped structures), and a simple perspective transformation (with 7 parameters: 3 translations; 3 rotations; and the SID). However, [19] does not model all sources of perspective distortion in a radiograph. In particular, the perspective transformation employed on that work does not model angled radiographs. In angled radiographs (e.g., Waters' view radiographs), the ray that joins the center of the image receptor and the X-ray generator is not perpendicular, resulting in a displacement of the principal point. This displacement causes perspective distortions. The method presented in [19] also showed the following drawbacks: (1) the robustness of the DE algorithm, especially with clavicles and patellae, that in some runs led to bad superimpositions due to the stochastic nature of DE and the highly multimodal search space tackled (see [19] for a study of the multimodal landscape of the problem); and (2) the large amount of time required to obtain a superimposition with DE (on average, 1800 seconds). This long time is motivated by the high computational time required by each evaluation (on average, it takes 0.250 seconds for a projection of 1290×1050 pixels in a standard computer), uncovering the computationally expensive optimization nature of the CR problem, and the high number of evaluations required by the optimizer to converge to a solution.

To overcome the aforementioned limitations, in this paper, we first extend the registration model (from a 7-DoF to a 9-DoF model) by including two more parameters to correct for perspective distortions (corresponding to the X and Y axis). This will allow us to model posterior-anterior and Waters' views for frontal sinuses. Second, we substitute DE by a RCEA specialized on expensive optimization real-coded problems (MVMO-SH).

III. Methodology

The evolutionary IR method requires the five following components (these are further detailed in [19] and depicted in Fig. 2): (1) the model (PM 3D surface model of the sinus cavity) and the scene image (AM radiograph, where the silhouette of the bone/cavity is segmented as well as the occlusion region, a.k.a. the region where the segmentation expert cannot distinguish if there is bone/cavity or not); (2) the perspective transformation responsible of generating a 2D image from a 3D object; (3) the expert knowledge of the problem that delimits the target transformation (i.e. radiographs acquisition protocols [36]); (4) a similarity metric which measures the resemblance of a 2D projection with the original 2D image (overlapping); and (5) a RCEA, which looks for the best parameters for the transformation to minimize the error of the similarity metric.

The projective transformation [37] behind an X-ray image is a perspective transformation with 9 parameters (6 extrinsic parameters: 3 translations; 3 rotations; and 3 intrinsic parameters: 1 SID and 2 movements of the principal point). Notice that in a radiograph the perspective distortion is mainly related to the source to SID [38] (see Figure 2) instead of the focal distance. However, angled radiographs, which are radiographs acquired with procedures where the ray that joins the X-ray generator and the center of the image receptor is not perpendicular, also have perspective distortions due to the movement of the principal point (see Fig. 2 for a graphical example).

Most works consider a calibrated scenario (only 6 parameters) and the SID is assumed as known which is not the case for the CR problem [31]. Although the perspective distortion can be small in many radiographs because of the large distance between the X-ray generator and receptor (as in chest radiographs), its consideration has shown to be crucial in the IR endeavour. This has been shown in [19], where better results were obtained using the perspective transformation than the orthographic transformation, despite the more challenging optimization problem involved.

The goodness of a projection of the PM 3D model with respect to fixed 2D segmentation of the radiograph is measured by a similarity metric, used as fitness function. This metric measures the resemblance of a 2D projection with the original 2D image (overlapping). The most utilized metric to measure the overlap of silhouettes is the DICE metric [35]. However, this metric is not robust against occlusion and does not allow partial matching. These drawbacks are overcome for the CR problem using the Masked DICE metric [19] (see eq. 1), designed ad-hoc for the CR problem. This metric incorporates the information of an occlusion region segmented by the expert into the DICE metric [35] increasing the robustness to occlusions and partial matching.

$$\text{Masked DICE} = \frac{2 \cdot |(I_A \setminus M) \cap (I_B \setminus M)|}{|I_A \setminus M| + |I_B \setminus M|} \quad (1)$$

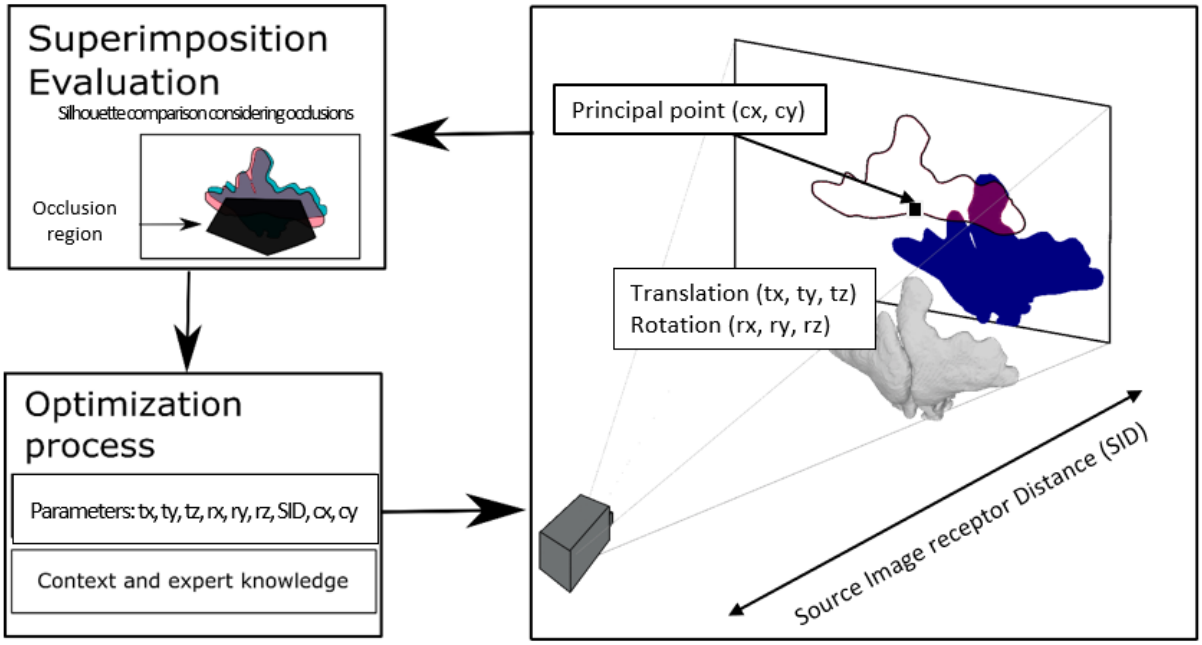

Fig. 2. Scheme of the proposal of 3D-2D IR for CR. Three main interconnected blocks are represented: (Right) the perspective transformation to obtain a projection of the 3D model with 9 parameters: translation (t_x, t_y, and t_z), rotation (r_x, r_y, and r_z), and perspective distortions (SID, β_x and β_y). In this figure, for the sake of clarity, we display distortions related to angled radiographs using the principal point. However, within the optimization process, instead of the location of this principal point we employ the angles of incidence of the principal ray on the center of the image receptor (β_x and β_y). These angles can be used to calculate the principal point displacement; (Top left) The similarity metrics that compares the PM projection (colored in blue) and the AM segmentation (colored in red) considering an occlusion region (colored in gray); (Bottom left) the optimization process to estimate the 9 parameters of the registration transformation that are only weakly limited by the context and expert knowledge from the X-ray acquisition protocol [36].

where I_A is the set of pixels of object A (segmented bone) silhouette, I_B is the set of pixels of object B (PM project bone) silhouette, and M is the occlusion region. Lastly, Gomez et. al [19] studied the complexity of the search space of CR showing the multi-modality of the CR problem even in its simplest version (synthetic cases without occlusions).

A. MVMO-SH

The search space of the perspective transformation is complex and highly multi-modal [19]. Therefore, classic numerical optimization methods are not sufficient, and more sophisticated techniques should be considered in order to solve it satisfactorily as RCEAs [33], [39].

The best real-coded evolutionary algorithm (RCEA) for solving computationally expensive real-coded optimization problems according to the IEEE CEC competitions is the mean-variance mapping optimization (MVMO) optimizer [20]. MVMO has ranked in top positions in expensive optimization competitions, such as IEEE CEC 2013 [21], 2014 [22], 2015 [23], 2016 [24], and 2018 [25], showing an excellent performance and robustness. MVMO is a novel single-individual RCEA that considers a best solution archive, but its novelty lies within a new mapping function employed for mutating the offspring. This mapping function is based on the mean and variance of the best solution archive. MVMO has been numerically compared to other enhanced RCEAs showing a better performance in many problems, especially in terms of convergence speed. For instance, a powerful memetic variant called MVMO-SH (the "S" refers to the offspring approach based on single parent and multi-parent crossover, and the "H" for the hybridization of MVMO with the use of local search (LS) [40]) improves the global search performance of the classical MVMO. MVMO-SH considers a set of solutions (i.e. particles of a swarm) instead of just one, each having its own best solution archive and mapping function, and allows the exchange of information and dynamic reduction of the swarm size.

MVMO-SH [21] begins with a initialization stage where the p particles (candidate solutions) of the swarm are randomly generated. The particles are normalized to the range [0, 1], which is a necessary condition to the latter mutation via mapping function (a key element in MVMO) and are only de-normalized for their fitness evaluation. Afterward, the following steps are performed for each generation (these are detailed in depth in [21]): (1) LS optimization of the particles with a probability p_{LS}; (2) If a particle founds a better solution in terms of fitness than those in its solution archive, the new solution is added to the particle's solution archive (notice that if the archive has reached its maximum size A_s the solution archive's worst solution is removed); (3) Particles are sorted and divided into two groups according to their fitness value, the GP best ones are classified as "good particles" and the rest as "bad particles" (GP is adapted along the process taking values between the 20% and 70% of p). The good particles are modified via a custom single parent crossover

operation based on local best [22] and bad particles via a custom multi-parent crossover operation based on a subset of good particles [22]; (4) the particles are mutated using a mapping function. This mapping function is based on the mean and variance of each particle's solution archive and a scaling factor f_s that modulates the function's shape. The scaling factor usually begins with a small value f_{start} and progressively increases until reaching its maximum value f_{end} to progressively increase the algorithm's accuracy.

To sum up, the most relevant parameters are: number of particles p (the recommended value is 15*$number\_variables$. If the number of particles chosen is equal to 1, MVMO-SH will perform as the standard MVMO), LS probability p_{LS}, archive size A_s, scaling factor start (f_{start}) and end values (f_{end}), initial value of the shape of all the variables at the beginning of the optimization d_r (values around 1-5 are suitable to guarantee good initial performance. In practice, it is usually set to 1), and parent selection method (random, neighbor group selection in single step or block steps, or sequential selection of the first variable and the rest randomly).

IV. Experiments

The experimental study is divided into two parts. The first experiment is devoted to the comparison of DE and MVMO-SH with simulated CR problems of frontal sinuses. Meanwhile, the second experiment is devoted to study the identification capability of the proposed IR framework using the best resulting RCEA in real images of frontal sinuses.

The same stopping criteria is established for the two RCEAs to allow a fair comparison in terms of computational resources. The optimization process ends when at least one of the following three conditions hold: (1) the maximum number of evaluations is reached. This value is set to 50,000 evaluations (it includes the evaluations performed by the LS methods); (2) the optimization process has got stuck. It is considered that the optimization process has stagnated when it has performed 10,000 evaluations without improving the fitness of the best solution; and (3) the optimization process has achieved a good solution/superimposition. A solution is considered of good quality when it shows an error lower than 0.001 in terms of fitness (i.e. the 99.9% of the pixels are correctly overlapped).

All experiments have been performed on the high-performance computing server Alhambra (Univ. of Granada), composed of 1808 cores Fujitsu PRIMERGY CX250/ RX350/RX500 nodes, although on average only 50 cores were available for this experimentation.

A. Performance metrics

Two ground truth (GT) metrics are employed to objectively measure the quality of the superimpositions achieved by the RCEAs: GT DICE [35] and the mean reprojection distance error (mRPD) [41]. The GT DICE metric measures the overlap between the GT projection's silhouette (equal to the simulated AM projection but without any occlusion) and the 2D projection's silhouette achieved by the RCEA. However, the GT DICE metric and the fitness function (i.e. Masked DICE) are highly correlated (e.g. they are equal in cases without occlusions) and thus, to avoid any possible bias, the mRPD metric is also employed. mRPD is a standard metric for the evaluation of 3D-2D IR methods by computing the reprojection error between the transformation obtained by the RCEA and the GT transformation (see [19] for further details of the utilization of mRPD in the CR problem). Notice that these metrics can be employed only in simulated CR problems since in real CR problems the GT projection and the GT transformation are unknown.

B. Experiment I: DE vs MVMO-SH on a simulated dataset

The dataset employed in Experiment I is formed by 150 simulated CR problems of frontal sinuses, each of them composed of a 3D surface model and a simulated radiograph of 480×600 pixels. All 3D surface models were manually segmented from CTs (see [19] for further details about the segmentation protocol). The simulated radiographs are randomly generated using a 9-DoFs perspective transformation within the ranges showed in Table I (these ranges have been set based on international acquisition protocols [36]). Each simulated radiograph has a different degree of occlusion in the frontal sinus silhouette: 50 simulated radiographs have no occlusion (0%); 50 simulated radiographs have an occlusion of around 20% of pixels; and the last 50 simulated radiographs have an occlusion of around 40% of pixels.

1) Experimental set-up: This experiment involves the application of the two optimizers (DE and MVMO-SH) using the 9-DoFs perspective distortions model. The parameters employed by both RCEAs are the following:

- DE: p = 100, F = 0.5, and P_c = 0.5 (tuned in [19]).
- MVMO-SH: p = d, A_s = 4, and F_{end} = 2.5 ([39]).

10 independent runs are performed to avoid any possible bias caused by the stochastic component of the optimizer, resulting in 3,000 runs/superimpositions and around 200 computation hours using 50 cores of the said infrastructure.

2) Results: As can be seen in Table II, the best results are clearly obtained by MVMO-SH. In all metrics, this optimizer yields better (or equally good) results than DE. Importantly, statistical tests to compare the performance of DE vs MVMO-SH were performed. The Wilcoxon rank sum test provided a p-value of 2.546e-13 (GT DICE) and 2.411e-15 (mRPD), showing the existence of statistically significant differences between the performance of both optimizers, in favor of MVMO-SH. Furthermore, MVMO-SH is more robust to occlusions in the silhouette of the skeletal structure than DE, showing a superb performance even with occlusions up to the 40% of silhouette (the maximum degree of occlusion evaluated). Regarding execution time to reach one of the three convergence criteria, DE presented an average, median and standard deviation execution time of 1665.0, 1440.2 and 913.1843 seconds, respectively. In turn, MVMO-SH took 1056.3, 1111.5 and 396.3469 seconds, respectively. Therefore, MVMO-SH is a better and faster optimizer for this particular problem.

DE converged 11,1% of executions, finished because it had obtained a good superimposition 17,1% of times, and

TABLE I
PARAMETER RANGE OF EACH SKELETAL STRUCTURE ACCORDING TO INTERNATIONAL ACQUISITION PROTOCOLS [36] AND EXPERT KNOWLEDGE. EACH MILLIMETER CORRESPONDS TO 2 PIXELS IN THE DIGITAL IMAGE DOMAIN.

Parameter	Frontal Sinuses
Image receptor dimension (mm)	240 × 300
t_x (mm)	[-125, 125]
t_y (mm)	[-150, 150]
t_z (mm)	[900 - 200, 900 + 200]
r_x, r_y, and r_z (degrees)	$[-40°, 40°]$
SID (mm)	[1000 - 100, 1000 + 100]
β_x (degrees)	[-10°, 10°]
β_y (degrees)	[-50°, 10°]

TABLE II
COMPARISON PERFORMANCE ACCORDING TO OPTIMIZER AND DEGREE OF OCCLUSION. THE LOWER THE VALUES THE BETTER.

Optimizer	Occlusion	Masked DICE			GT DICE			mRPD		
		mean	median	std	mean	median	std	mean	median	std
DE	0	0.004	**0.001**	0.026	0.004	**0.001**	0.026	0.137	0.031	1.122
	20	0.008	**0.001**	0.036	0.013	**0.002**	0.041	0.307	0.051	1.405
	40	0.012	**0.001**	0.038	0.029	0.004	0.065	0.476	0.079	1.601
MVMO-SH	0	**0.002**	**0.001**	**0.016**	**0.002**	**0.001**	**0.016**	**0.056**	**0.021**	**0.640**
	20	**0.001**	**0.001**	**0.001**	**0.002**	**0.002**	**0.001**	**0.039**	**0.035**	**0.023**
	40	**0.001**	**0.001**	**0.001**	**0.003**	**0.002**	**0.002**	**0.046**	**0.041**	**0.026**

achieved the maximum number of evaluations 71,8% of times. MVMO-SH converged 21,4% of executions, obtained a good superimposition 78,6% of times, and it never needed to achieve the maximum number of evaluations.

C. Experiment II: Identification capability of our 3D-2D IR-based CR framework with frontal sinuses on real data

The dataset employed was provided by the *Hospital de Castilla-La Mancha* (Spain) and is composed of 50 CTs and 50 radiographs where the frontal sinuses are visible. All CTs and radiographs were manually segmented by two MSc students (José Manuel Pérez Jiménez and Andrea Cerezo Vallecillo), both from the Physical Anthropology lab of Univ. of Granada.

1) Experimental set-up: This experiment studies the identification capability of the proposed 3D-2D IR-based CR framework using frontal sinuses and the best RCEA (MVMO-SH). We have performed a radiograph inter-expert study, where we have compared the two segmentations performed by the two aforementioned forensic experts on 50 radiographs against 50 CTs. In this experiment, we have only used the segmentation of the CTs performed by one of the MSc students, since the inter-expert segmentation error in CTs was practically non-existent. A total of 2,500 cross comparisons per segmentation.

Since previous experiments have already shown the robustness of MVMO-SH, and due to the large computational cost of employing again 10 repetitions, only 2 independent runs are performed. Each of the 5,000 runs takes on average 1,000 seconds, resulting in 2,777 hours of computation (or 166 computation days) that, performed on the 50 available cores of computing server Alhambra, required "only" around 56 computation hours (3 computation days).

2) Results: Positive and negative cases have shown important differences in terms of fitness according to the Masked DICE Metric (see Fig. 3). However, this metric alone is not sufficient to precisely distinguish between positive and negative cases. Therefore, the results are reported using Cumulative Match Characteristic (CMC) curves (see Fig. 4) to study the identification capabilities of the proposal as done in [42] and in [19]. To focus on the identification reliability of the method only the best run (out of two) of each experiment is considered.

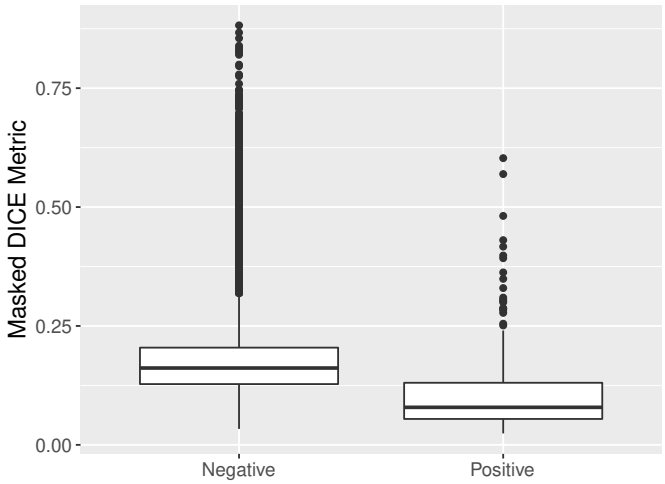

Fig. 3. Boxplots of the minimum error of positive and negative cases according to the Masked DICE metric.

Regardless of the X-ray image segmentation employed (see Fig. 4), the positive case ranks in the first position at least

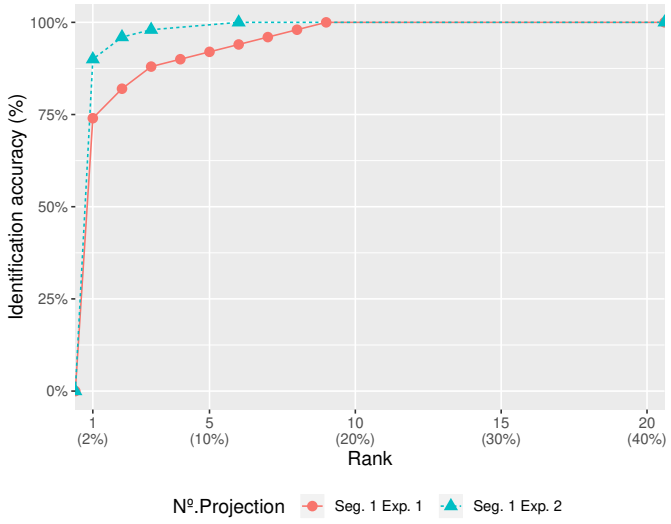

Fig. 4. CMC curves of the radiograph inter-expert study (2 segmentations performed by 2 anthropologists; 50×50 comparisons per segmentation)

75% of the cross-comparisons (out of 50 candidates, 2% of the total sample). Furthermore, it reaches a confidence level of 100% of success when considering the first nine positions (18% of the sample). One direct implication of this result is that the current framework, based only on the value of the Masked DICE metric, is able to filter out 82% of the possible candidates with 0 error rate in a fully automatic manner. Furthermore, the superimposition framework is robust to inter-expert segmentation errors in radiographs, since results hardly vary between segmentations.

V. Conclusions

This paper presents an automatic frontal sinuses IR method in CR using RCEAs. The task is formulated as a 3D-2D IR problem using a 9-DoF perspective transformation model. Two RCEAs (DE and MVMO-SH) are compared in the minimization of the registration cost function, and the best of them (MVMO-SH) is applied to an identification scenario including 50 X-ray images and 50 CTs. The results obtained show that the proposed automatic identification system is able to filter more than 80% of the sample, reducing time and costs in the posterior application of other identification techniques (e.g., DNA analysis) to a reduced candidates list. This paper presents an automatic identification system with regard to the calculation of the overlap of AM and PM materials. But the previous segmentation of these materials is given (i.e., it is manually obtained). As immediate future work it is necessary to integrate an automatic segmentation approach, for which there are already effective methods [43], and to verify the identification power of the complete system. We also plan to perform inter-expert and intra-expert studies to investigate the robustness of our method to segmentation errors, specially in the upper border. In the long term, we propose to implement and validate a hierarchical forensic identification decision support system that integrates different criteria, superimpositions, and skeletal structures.

Acknowledgment

This work was supported by the Spanish Ministry of Science, Innovation and Universities, and European Regional Development Funds (ERDF) under grant EXASOCO (PGC2018-101216-B-I00), and by the Regional Government of Andalusia under grant EXAISFI (P18-FR-4262). Mr. Gómez's work was supported by Spanish MECD FPU grant [grant number FPU14/02380]. Pablo Mesejo is funded by the European Commission H2020-MSCA-IF-2016 through the Skeleton-ID Marie Curie Individual Fellowship [reference 746592]. Drs. Ibáñez and Valsecchi's work is funded by Spanish Ministry of Science, Innovation and Universities-CDTI, Neotec program 2019 [reference EXP-00122609/SNEO-20191236].

References

[1] M. J. Thali, B. Brogdon, M. D. Viner, Forensic radiology, CRC Press, 2002.
[2] W. C. Roentgen, On a new kind of rays, Br J Radiol 4 (1895) 32–153.
[3] R. C. Kirkpatrick, The New Photography: with Report of a Case in which a Bullet was Photographed in the Leg, Montreal, 1984.
[4] P. C. Goodman, The new light: discovery and introduction of the x-ray., AJR. American Journal of Roentgenology 165 (5) (1995) 1041–1045.
[5] B. G. Brogdon, J. E. Lichtenstein, Forensic radiology in historical perspective, Critical Reviews in Diagnostic Imaging 41 (1) (2000) 13–42.
[6] A. C. Singleton, The roentgenological identification of victims of the "noronic" disaster, The American Journal of Roentgenology and Radium Therapy 66 (3) (1951) 375—384.
[7] E. Streetman, T. W. Fenton, Chapter 22 - comparative medical radiography: Practice and validation, in: K. E. Latham, E. J. Bartelink, M. Finnegan (Eds.), New Perspectives in Forensic Human Skeletal Identification, Academic Press, 2018, pp. 251 – 264. doi:https://doi.org/10.1016/B978-0-12-805429-1.00022-3.
[8] T. Kahana, J. Hiss, Identification of human remains: forensic radiology, Journal of Clinical Forensic Medicine 4 (1) (1997) 7–15.
[9] A. M. Christensen, G. M. Hatch, Advances in the use of frontal sinuses for human identification, in: New Perspectives in Forensic Human Skeletal Identification, Elsevier, 2018, pp. 227–240.
[10] G. Cossellu, S. De Luca, R. Biagi, G. Farronato, M. Cingolani, L. Ferrante, R. Cameriere, Reliability of frontal sinus by cone beam-computed tomography (CBCT) for individual identification, La Radiologia Medica 120 (12) (2015) 1130–1136.
[11] A. L. Vickers, Daubert, critique and interpretation: What empirical studies tell us about the application of daubert, USFL Rev. 40 (2005) 109.
[12] N. J. Kirk, R. E. Wood, M. Goldstein, Skeletal identification using the frontal sinus region: a retrospective study of 39 cases, Journal of Forensic Sciences 47 (2) (2002) 318–323.
[13] W. L. Culbert, F. M. Law, Identification by comparison of roentgenograms: of nasal accessory sinuses and mastoid processes, Journal of the American Medical Association 88 (21) (1927) 1634–1636.
[14] M. Yoshino, S. Miyasaka, H. Sato, S. Seta, Classification system of frontal sinus patterns by radiography. its application to identification of unknown skeletal remains, Forensic Science International 34 (4) (1987) 289–299.
[15] R. F. da Silva, F. B. Prado, I. G. C. Caputo, K. L. Devito, T. de Luscena Botelho, E. D. Júnior, The forensic importance of frontal sinus radiographs, Journal of Forensic and Legal Medicine 16 (1) (2009) 18–23.
[16] D. Gibelli, M. Cellina, A. Cappella, S. Gibelli, M. M. Panzeri, A. G. Oliva, G. Termine, D. De Angelis, C. Cattaneo, C. Sforza, An innovative 3D-3D superimposition for assessing anatomical uniqueness of frontal sinuses through segmentation on CT scans, International Journal of Legal Medicine 133 (4) (2019) 1159–1165.

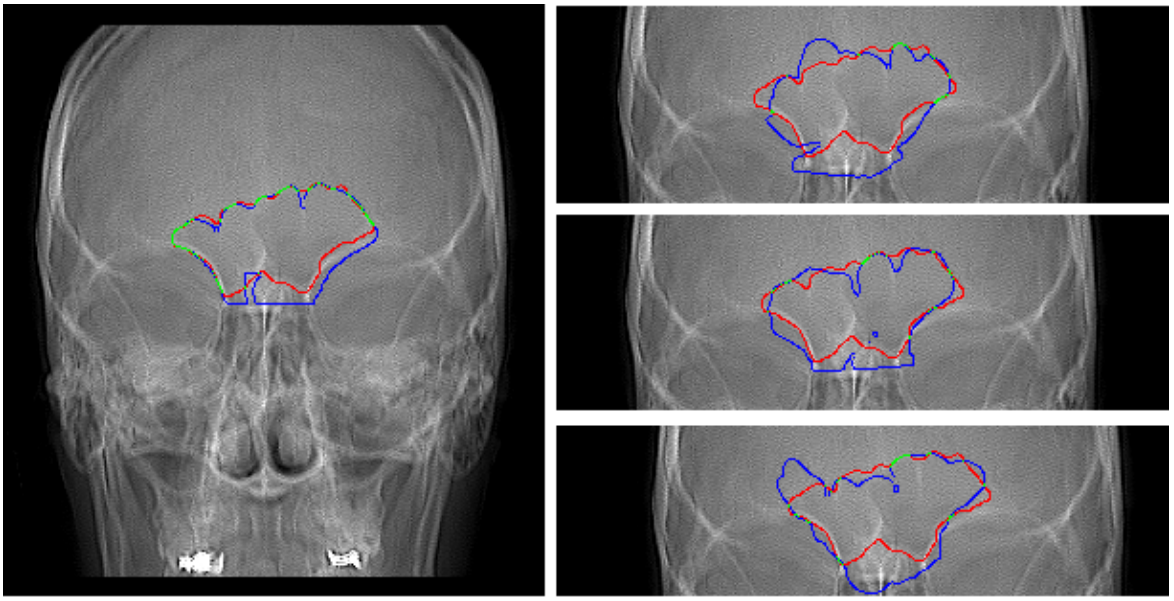

Fig. 5. (Left) An example of a positive case, radiograph A compared against CT A; (Right) Example of negative cases, radiograph A compared against CTs A, B and C. Red lines display the segmented X-ray AM image, blue lines represent the projected 3D PM image (i.e., the registration result, or silhouette that we try to align to the red one), green lines represent perfect overlap between red and blue lines.

[17] B. H. D. Gerard J. Tortora, Principles of Anatomy and Physiology [With A Brief Atlas of the Skeleton, Surface Anatomy], 12th Edition, Wiley, 2008.

[18] P. Markelj, D. Tomaževič, B. Likar, F. Pernuš, A review of 3D/2D registration methods for image-guided interventions, Medical Image Analysis 16 (3) (2012) 642–661.

[19] O. Gómez, O. Ibáñez, A. Valsecchi, O. Cordón, T. Kahana, 3D-2D silhouette-based image registration for comparative radiography-based forensic identification, Pattern Recognition 83 (2018) 469–480.

[20] I. Erlich, G. K. Venayagamoorthy, N. Worawat, A mean-variance optimization algorithm, in: 2010 IEEE Congress on Evolutionary Computation (CEC), 2010, pp. 1–6.

[21] J. L. Rueda, I. Erlich, Hybrid mean-variance mapping optimization for solving the IEEE-CEC 2013 competition problems, in: 2013 IEEE Congress on Evolutionary Computation (CEC), 2013, pp. 1664–1671.

[22] I. Erlich, J. L. Rueda, S. Wildenhues, F. Shewarega, Solving the IEEE-CEC 2014 expensive optimization test problems by using single-particle MVMO, in: 2014 IEEE Congress on Evolutionary Computation (CEC), IEEE, 2014, pp. 1084–1091.

[23] J. L. Rueda, I. Erlich, MVMO for bound constrained single-objective computationally expensive numerical optimization, in: 2015 IEEE Congress on Evolutionary Computation (CEC), IEEE, 2015, pp. 1011–1017.

[24] J. L. Rueda Torres, I. Erlich, Solving the CEC2016 real-parameter single objective optimization problems through MVMO-PHM, in: 2016 IEEE World Congress on Computational Intelligence, 2016, pp. 1–10.

[25] J. L. Rueda, I. Erlich, Hybrid single parent-offspring MVMO for solving CEC2018 computationally expensive problems, in: 2018 IEEE Congress on Evolutionary Computation (CEC), IEEE, 2018, pp. 1–8.

[26] S. Damas, O. Cordón, O. Ibáñez, J. Santamaría, I. Alemán, M. Botella, F. Navarro, Forensic identification by computer-aided craniofacial superimposition: a survey, ACM Computing Surveys 43 (4) (2011) 1–27.

[27] A. M. Christensen, Testing the reliability of frontal sinuses in positive identification, Journal of Forensic Sciences 50 (1) (2005) 18–22.

[28] C. N. Stephan, B. Amidan, H. Trease, P. Guyomarc'h, T. Pulsipher, J. E. Byrd, Morphometric comparison of clavicle outlines from 3D bone scans and 2D chest radiographs: a shortlisting tool to assist radiographic identification of human skeletons, Journal of Forensic Sciences 59 (2) (2014) 306–313.

[29] E. Niespodziewanski, C. N. Stephan, P. Guyomarc'h, T. W. Fenton, Human identification via lateral patella radiographs: A validation study, Journal of Forensic Sciences 61 (1) (2016) 134–140.

[30] J. Caple, J. Byrd, C. N. Stephan, Elliptical fourier analysis: fundamentals, applications, and value for forensic anthropology, International Journal of Legal Medicine 131 (6) (2017) 1675–1690.

[31] D. B. Russakoff, T. Rohlfing, K. Mori, D. Rueckert, A. Ho, J. R. Adler, C. R. Maurer, Fast generation of digitally reconstructed radiographs using attenuation fields with application to 2D-3D image registration, IEEE Transactions on Medical Imaging 24 (11) (2005) 1441–1454.

[32] J. Feldmar, N. Ayache, F. Betting, 3D-2D projective registration of free-form curves and surfaces, in: Proceedings of the Fifth International Conference on Computer Vision 1995, IEEE, 1995, pp. 549–556.

[33] S. Damas, O. Cordón, J. Santamaría, Medical image registration using evolutionary computation: An experimental survey, IEEE Computational Intelligence Magazine 6 (4) (2011) 26–42.

[34] R. Storn, K. Price, Differential evolution–a simple and efficient heuristic for global optimization over continuous spaces, Journal of Global Optimization 11 (4) (1997) 341–359.

[35] T. Sørensen, A method of establishing groups of equal amplitude in plant sociology based on similarity of species and its application to analyses of the vegetation on danish commons, Kongelige Danske Videnskabernes Selskab 5 (1948) 1–34.

[36] K. L. Bontrager, J. Lampignano, Textbook of radiographic positioning and related anatomy, Elsevier Health Sciences, 2013.

[37] R. Hartley, A. Zisserman, Multiple view geometry in computer vision, Cambridge University Press, 2003.

[38] D. Mery, X-ray Testing, Springer International Publishing, Cham, 2015, pp. 1–33.

[39] O. Gómez, Soft computing y visión por ordenador para la identificación forense mediante comparación de radiografías, Ph.D. thesis, Universidad de Granada (2020).

[40] R. H. Byrd, J. C. Gilbert, J. Nocedal, A trust region method based on interior point techniques for nonlinear programming, Mathematical programming 89 (1) (2000) 149–185.

[41] E. B. van de Kraats, G. P. Penney, D. Tomazevic, T. Van Walsum, W. J. Niessen, Standardized evaluation methodology for 2-D-3-D registration, IEEE Transactions on Medical Imaging 24 (9) (2005) 1177–1189.

[42] C. Campomanes-Alvarez, O. Ibáñez, O. Cordón, C. Wilkinson, Hierarchical information fusion for decision making in craniofacial superimposition, Information Fusion 39 (2018) 25–40.

[43] O. Gómez, P. Mesejo, O. Ibáñez, A. Valsecchi, O. Cordón, Deep architectures for high-resolution multi-organ chest X-ray image segmentation, Neural Computing and Applications (2020, In Press) 1–15.